

Spectral energy distributions and age estimates of 40 massive young stellar objects

K. K. Tanti^{1}, J. Roy², K. Duorah¹*

¹Department of Physics, Gauhati University, Guwahati, 781014, Assam, India

²Indian Institute of Astrophysics, Bangalore, 560034, India

In this paper, we present the spectral energy distributions (SEDs) of 40 massive young stellar objects (YSOs), detected from the NIR imaging survey carried out by Varricatt et al. 2010 and estimated their ages and masses. The SEDs of YSOs in 40 massive star forming regions have been reconstructed using 2MASS, MSX, IRAS, IRAC & MIPS, SCUBA, WISE, SPIRE and IRAM data, partly available from previous works, using the on-line `SED Fitting tool (SED Fitter)` developed by Robitaille et al. 2006, 2007. Apart from IRAS catalogue fluxes, the fluxes in the Mid-IR and sub-mm/mm were derived directly from the images. With the help of the analysis of SEDs, we have extracted important physical and structural parameters for each of the massive young stellar objects, along with the associated circumstellar disk and envelope. The cumulative distribution of the stellar ages and masses of the massive YSOs lead to a scenario for the formation history of massive stars in their respective star forming regions.

Key words: stars: massive, stars: pre-main-sequence, radiative transfer

INTRODUCTION

The formation and the initial stages of the evolution of massive stars in our galaxy take place inside dense regions within molecular clouds, from which they are born. This process deals with the protostars/YSOs in the environment of interstellar gas and dust from the parent cloud. In this environment, the young stellar objects and protostars are associated with circumstellar dust and molecular gas, which absorbs the stellar radiation and re-emits it to wavelengths long wards than $1\mu\text{m}$ [3]. According to [3], the protostars have a SED with a positive slope in the 2-20 μm spectral range. By the shapes of the SEDs, [3] first classified pre-main sequence (PMS) stars into an evolutionary sequence, Classes I through III (later an earlier stage, Class 0 was also proposed to describe more deeply embedded sources). This has been proved for low mass YSOs [2]. The case for young massive stars is topic of recent investigation [11].

To understand the pre-main sequence evolution processes of the stars, the study of the circumstellar environment of YSOs is crucial. For this, multi-wavelength photometry can be done and subsequently, the SEDs can be constructed by computing the radiation transfer models, considering given circumstellar dust and gas geometry, as well as dust properties, and thus finding a set of parameters that

reproduce the observations.

SED MODEL FITTING

In order to characterise the physical properties and the evolutionary status of disks and envelopes around all the selected 40 YSO outflow sources, the SEDs of YSOs were modelled using on-line `SED Fitting Tool` of [5], that uses a grid of 2D radiative transfer models presented in [4], developed by [9, 10]. To obtain better results for constructing SEDs for all sources, we compiled and used all the available NIR, MIR and FIR data, e.g., 2MASS J-H-K_s band data, magnitudes in the Spitzer IRAC bands 1-4 & MIPS bands 1-2, IRAS 12, 25, 60, 100- μm data, MSX Bands A, C, D & E data, SCUBA 450 & 850- μm data, WISE 3.4, 4.6, 12, 22- μm data, SPIRE 250, 350, 500- μm data and the IRAM 1.2 mm data.

SELECTION OF YSOs

We selected intermediate and massive young stellar outflow candidates from the NIR imaging survey carried out in [7]. The reason for selecting these outflow candidates is that bipolar molecular outflows have long indicated that accretion discs are present at the heart of massive star formation. In [7] those candidates that are young, high-mass objects with evidence of outflows, were selected.

*research.kamal@gmail.com

DISCUSSION

As stars form and evolve following an evolutionary sequence, physical and structural properties of YSOs also evolve. Fitting their SEDs can provide us these properties, which can give us insights to understand the physical and structural evolution of pre-main sequence stars as well as the evolution of star clusters where these massive stars were born. The physical properties of the central source, such as effective temperature and luminosity, are the most important parameters in understanding the evolutionary status of the central source, and play a crucial role in the physical properties of disks and envelopes, because dust in the disks and envelopes are heated by irradiation from the star and from accretion shocks at the stellar surface [6].

The physical and structural parameters of all the 40 intermediate and massive YSO outflow candidates, along with the associated circumstellar disk and envelope, are obtained with the help of SED Fitting Tool.

The stellar masses, stellar ages, stellar temperatures and total luminosities of all the central YSO sources are shown in Table 1. The best-fit model SEDs for few selected massive YSO outflow sources, viz. IRAS 18144-1723, IRAS 18345-0641, IRAS 19217+1651, IRAS 19410+2336, IRAS 21519+5613 & IRAS 22305+5803, are shown in Fig. 1. Out of all the 40 target sources, 27 are calculated as massive YSOs, ranging from $8.18 M_{\odot}$ to $28.6 M_{\odot}$, whereas 13 are low and intermediate-mass YSOs, ranging from $2.51 M_{\odot}$ to $7.92 M_{\odot}$. The stellar temperatures of the sources are ranging from 4149 K to 24558 K. The stellar ages of all the sources are calculated. For the 13 intermediate YSO outflow candidates, the stellar ages are ranging from 1.82×10^3 yr to 8.79×10^5 yr. In case of massive YSO outflow candidates, the stellar ages range from 1.24×10^3 yr to 9.80×10^5 yr. Similarly, the envelopes that surrounded the central YSO sources are large with mass range of $6.12 M_{\odot}$ – $4.14 \times 10^3 M_{\odot}$, whereas envelope radii range between 1.13×10^4 AU – 1.00×10^5 AU. The estimated envelope accretion rates are high with a range of $4.83 \times 10^{-8} M_{\odot}/\text{yr}$ – $9.71 \times 10^{-3} M_{\odot}/\text{yr}$. The large envelope size signifies that the accretion is spherical on the size-scales of dense cores [1]. Also, we have estimated the range of disk parameters as follows: disk mass: $5.69 \times 10^{-4} M_{\odot}$ – $4.64 \times 10^{-1} M_{\odot}$; disk radius: 3.79 AU – 1.91×10^3 AU; disk accretion rate: $1.52 \times 10^{-9} M_{\odot}/\text{yr}$ – $3.32 \times 10^{-4} M_{\odot}/\text{yr}$. In the current study, every SED model showed a disk for each YSO, but at the same time, this SED model may not be sensitive towards the presence or absence of this

disk — because in an accretion scenario, envelope flux always overpowers the disk flux.

Considering the most massive among the sample of 40 individual central YSO sources, i.e., IRAS 19110+1045, for which we have estimated the physical parameters as: stellar mass = $28.60 M_{\odot}$, stellar radius = $53.62 R_{\odot}$, stellar temperature = 14052 K, stellar age = 5.74×10^3 yr and total luminosity = $1.01 \times 10^5 L_{\odot}$.

Using an older self-consistent radiative transfer modelling technique, in [8] the total luminosity as $3.3 \times 10^5 L_{\odot}$, for IRAS 19110+1045, was estimated by integrating the observed SED, whereas the total luminosity of the resolved stars is $1.1 \times 10^5 L_{\odot}$. From the SED, that shows a higher composition of silicate (60%) grains, they also estimated the other parameters as: dust mass = $450 M_{\odot}$, the gas to dust ratio by mass = 450, cold dust mass = $30 M_{\odot}$, gas mass = $1.3 \times 10^4 M_{\odot}$.

In [1] the physical properties of the infrared counterparts of 380 high mass protostellar objects were estimated and analysed by using their spectral energy distributions (SED) predicted by radiative transfer accretion models of YSOs, that successfully explained a YSO accretion model which further represent a realistic picture of massive star formation. Using the results in the current study, we can understand the physical and structural evolution of the YSOs taken into consideration which will self-consistently explain the embedded young stellar objects (YSO) in dense interstellar clouds, which will lead to a scenario for the formation history of massive stars in their respective star forming regions.

REFERENCES

- [1] Grave J. M. C. & Kumar M. S. N. 2009, A&A, 498, 147
- [2] Hartmann L., Megeath S. T., Allen L. et al. 2005, ApJ, 629, 881
- [3] Lada C. J. 1987, in IAU Symposium, 115, 1
- [4] Robitaille T. P., Whitney B. A., Indebetouw R., Wood K. & Denzmore P. 2006, ApJS, 167, 256
- [5] Robitaille T. P., Whitney B. A., Indebetouw R. & Wood K. 2007, ApJS, 169, 328
- [6] Sung H. & Bessell M. S. 2010, AJ, 140, 2070
- [7] Varricatt W. P., Davis C. J., Ramsay S. & Todd S. P. 2010, MNRAS, 404, 661
- [8] Vig S., Ghosh S. K., Kulkarni V. K., Ojha D. K. & Verma R. P. 2006, ApJ, 637, 400
- [9] Whitney B. A., Wood K., Bjorkman J. E. & Cohen M. 2003, ApJ, 598, 1079
- [10] Whitney B. A., Wood K., Bjorkman J. E. & Wolff M. J. 2003, ApJ, 591, 1049
- [11] Zinnecker H. & Yorke H. W. 2007, ARA&A, 45, 481

Table 1: The stellar masses, stellar ages, stellar temperatures and total luminosities of the 40 intermediate and massive young stellar objects.

Sl No.	YSO Source	Stellar Age (yr)	Stellar Mass (M_{\odot})	Stellar Temperature (K)	Total Luminosity (L_{\odot})
1	IRAS 00420+5530	$1.36 \cdot 10^4$	12.61	6332	$6.37 \cdot 10^3$
2	IRAS 04579+4703	$1.32 \cdot 10^5$	7.31	7218	$9.32 \cdot 10^2$
3	IRAS 05137+3919	$1.53 \cdot 10^5$	7.78	12660	$3.05 \cdot 10^3$
4	IRAS 05168+3634	$5.93 \cdot 10^3$	14.44	4502	$7.65 \cdot 10^3$
5	IRAS 05274+3345	$7.87 \cdot 10^5$	6.39	19338	$1.81 \cdot 10^3$
6	IRAS 05358+3543	$6.03 \cdot 10^4$	8.18	6325	$1.14 \cdot 10^3$
7	IRAS 05373+2349	$4.36 \cdot 10^3$	2.51	4167	$4.86 \cdot 10^2$
8	IRAS 05490+2658	$1.60 \cdot 10^5$	7.31	8858	$1.27 \cdot 10^3$
9	IRAS 05553+1631	$5.40 \cdot 10^3$	9.36	4428	$1.50 \cdot 10^3$
10	IRAS 06061+2151	$2.89 \cdot 10^4$	11.21	8479	$4.72 \cdot 10^3$
11	IRAS 06584-0852	$8.27 \cdot 10^5$	6.61	19796	$1.33 \cdot 10^3$
12	IRAS 18144-1723	$2.10 \cdot 10^4$	15.44	14321	$2.22 \cdot 10^4$
13	IRAS 18159-1648	$3.13 \cdot 10^5$	7.70	21221	$2.52 \cdot 10^3$
14	IRAS 18174-1612	$6.77 \cdot 10^3$	20.11	9139	$2.97 \cdot 10^4$
15	IRAS 18182-1433	$1.60 \cdot 10^4$	21.76	23884	$7.79 \cdot 10^4$
16	IRAS 18264-1152	$1.53 \cdot 10^4$	10.64	5117	$3.24 \cdot 10^3$
17	IRAS 18345-0641	$1.36 \cdot 10^4$	12.99	6733	$7.21 \cdot 10^3$
18	IRAS 18360-0537	$8.79 \cdot 10^5$	5.70	17951	$7.76 \cdot 10^2$
19	IRAS 18385-0512	$2.93 \cdot 10^4$	10.05	6681	$2.92 \cdot 10^3$
20	IRAS 18517+0437	$1.24 \cdot 10^3$	11.77	4149	$4.68 \cdot 10^3$
21	IRAS 19092+0841	$1.36 \cdot 10^4$	12.99	6733	$7.21 \cdot 10^3$
22	IRAS 19110+1045	$5.74 \cdot 10^3$	28.60	14052	$1.01 \cdot 10^5$
23	IRAS 19213+1723	$1.67 \cdot 10^5$	7.92	15821	$4.34 \cdot 10^3$
24	IRAS 19217+1651	$8.11 \cdot 10^3$	13.67	5066	$8.20 \cdot 10^3$
25	IRAS 19374+2352	$9.13 \cdot 10^3$	11.11	4564	$3.03 \cdot 10^3$
26	IRAS 19388+2357	$1.82 \cdot 10^3$	6.47	4153	$7.32 \cdot 10^2$
27	IRAS 19410+2336	$7.77 \cdot 10^4$	10.10	17996	$9.06 \cdot 10^3$
28	IRAS 20050+2720	$4.03 \cdot 10^3$	7.83	4268	$1.02 \cdot 10^3$
29	IRAS 20188+3928	$3.17 \cdot 10^4$	9.87	6785	$2.74 \cdot 10^3$
30	IRAS 20198+3716	$9.80 \cdot 10^5$	8.99	24325	$4.31 \cdot 10^3$
31	IRAS 20227+4154	$5.32 \cdot 10^5$	6.98	20519	$1.64 \cdot 10^3$
32	IRAS 20062+3550	$4.03 \cdot 10^3$	7.83	4268	$1.02 \cdot 10^3$
33	IRAS 20293+3952	$2.03 \cdot 10^4$	10.91	6198	$3.83 \cdot 10^3$
34	IRAS 21307+5049	$1.05 \cdot 10^5$	8.26	10875	$2.82 \cdot 10^3$
35	IRAS 21391+5802	$5.86 \cdot 10^4$	2.99	4389	$8.08 \cdot 10^1$
36	IRAS 21519+5613	$6.74 \cdot 10^4$	11.69	24558	$1.51 \cdot 10^4$
37	IRAS 22172+5549	$2.93 \cdot 10^4$	10.05	6681	$2.92 \cdot 10^3$
38	IRAS 22305+5803	$2.80 \cdot 10^4$	10.55	7216	$3.54 \cdot 10^3$
39	IRAS 22570+5912	$7.77 \cdot 10^4$	10.10	17996	$9.06 \cdot 10^3$
40	IRAS 23139+5939	$8.59 \cdot 10^5$	6.79	20138	$1.55 \cdot 10^3$

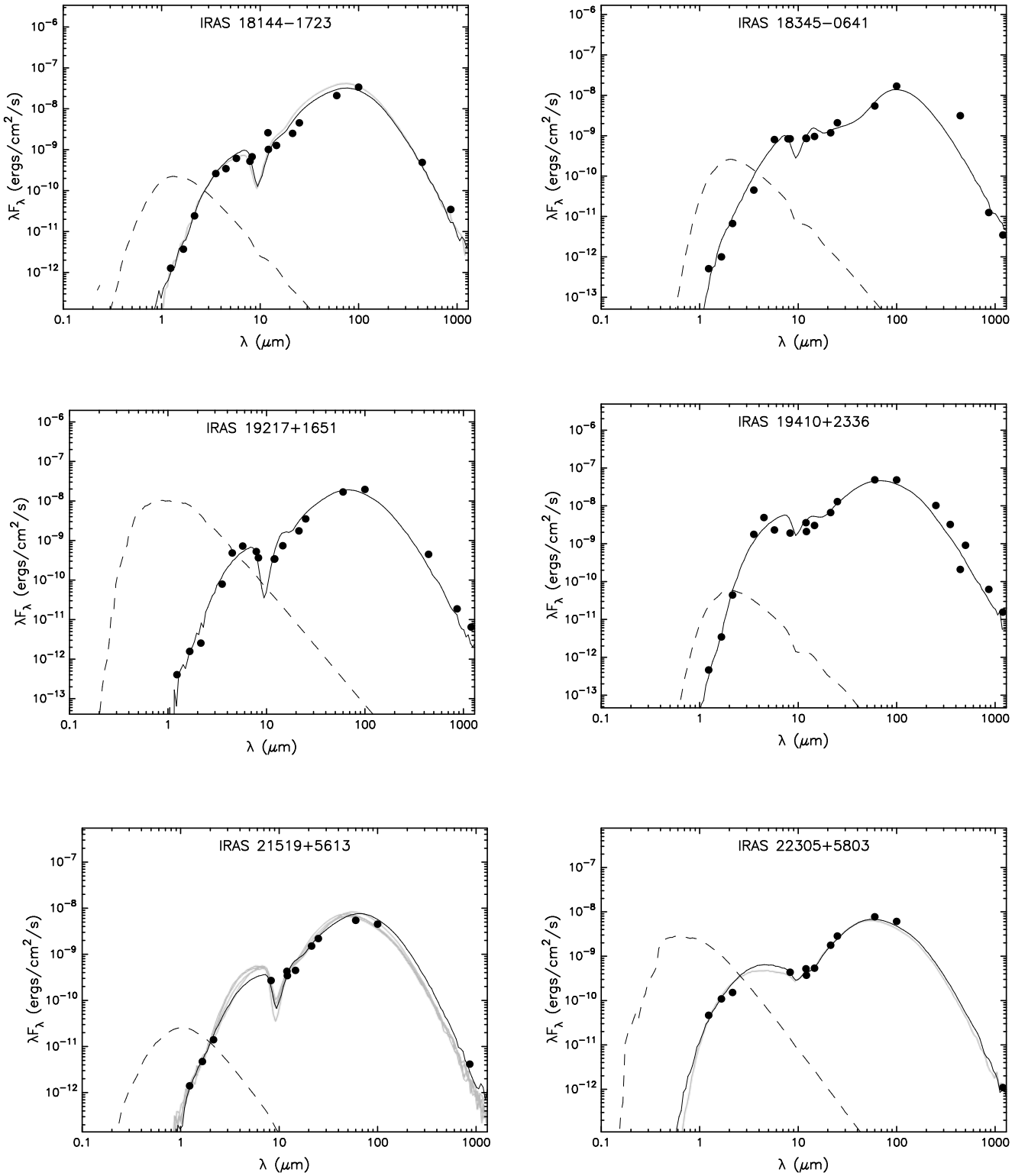


Fig. 1: The best-fit model SEDs of IRAS 18144-1723, IRAS 18345-0641, IRAS 19217+1651, IRAS 19410+2336, IRAS 21519+5613 and IRAS 22305+5803.